16th World Conference on Earthquake, 16WCEE 2017

Santiago Chile, January 9th to 13th 2017

Paper N° 1161

Registration Code: S-U1461982307

STUDY ON THE REASONABLE LIQUEFACTION PREDICTION IN CASE OF THE HUGE INTERPLATE EARTHQUAKE BASED ON THE REPRESENTATIVE SOIL PROFILE MODELS

K. Ishikawa(1), S. Yasuda(2)

(1) *Assistant Professor, Tokyo Denki University, ishikawa@g.dendai.ac.jp*
(2) *Vice President, Tokyo Denki University, yasuda@g.dendai.ac.jp*

Abstract

The 2011 Great East Japan Earthquake, with a magnitude of MW = 9.0, occurred in the Pacific Ocean about 130 km off the northeast coast of Japan's main island on March 11, 2011. The epicentral distance was very long, about 380 to 400 km, and liquefaction occurred over a wide area of reclaimed land along Tokyo Bay. The most seriously damaged area was Urayasu City, where about 85% of the area was liquefied. Seismic intensities in the liquefied zones were not high, although the liquefied grounds were covered with boiled sand. Most likely, the very long duration of the main shock along with the large aftershock that hit 29 min later induced the severe liquefaction. When discussing the prediction and the countermeasure to liquefaction at future, it is necessary to consider the influence of the very long duration earthquake motion of a huge interplate earthquake. In Japan, the liquefaction prediction procedure is categorized as a technique for civil engineering structures and buildings. In the method for civil engineering structures, weighting factors for earthquake motion characteristics are provided for interplate and inland earthquakes.

The objective of this study was to perform reasonable prediction of a huge interplate earthquake, including the seismic effects of long duration and the regionality of liquefaction strength using Representative Soil profile models created from existing ground survey results. The study area is Urayasu which suffered the most serious liquefaction damage. This area is divided into the reclaimed land which liquefied, and the natural deposition ground which is not liquefied. A ground model is the Representative Soil Profile Models which equalized the existing ground survey results in 250 m meshes.

In order to carry out reasonable liquefaction prediction in case of a huge interplate earthquake, it was confirmed that it is necessary to take into consideration the regionality of a liquefaction strength ratio and the influence of a long-time continuation earthquake motion. The Confirm of the matching property with the real damage of a prediction result uses the fieldwork results after the earthquake due to Chiba Prefecture. In this fieldwork, the distribution of the amount of relative displacements of the structures on the pile foundation and a ground surface is obtained in detail. A liquefaction potential of the degree index of liquefaction is obtained from a liquefaction prediction result by integrating with a distribution of the depth direction of a safety factor against liquefaction. A liquefaction potential and the amount of ground-surface relative displacements tend to increase similarly, and were able to confirm the prediction result and the matching property of the real damage.

Keywords: Liquefaction prediction, Large interplate earthquake, Representative Soil Profile Models

1. Introduction

The 2011 Great East Japan Earthquake, with a magnitude of M_W = 9.0, occurred in the Pacific Ocean approximately 130 km off the northeast coast of Japan's main island on March 11, 2011. The epicentral distance was very large, 380 to 400 km, and liquefaction occurred over a wide area of reclaimed land along Tokyo Bay. The most seriously damaged area was Urayasu City, where approximately 85% of the area was liquefied. Typical liquefaction-induced damages of reclaimed land are the settlement and tilting of timbered houses, disconnection of water and gas service pipes, and breakage of sewer pipes. The observed values of earthquake motion in the Tokyo Bay coast area, including Urayasu, are shown in Fig.1. Seismic intensities in the liquefied zones were not high, although liquefied ground was covered with boiled sand. Most likely, the very long duration of the main shock, along with the large aftershock that hit 29 min later, induced the severe liquefaction. When discussing liquefaction prediction and countermeasures in the future, it will be necessary to consider the effect of long motion duration by a huge interplate earthquake.

In Japan, the liquefaction prediction procedure is categorized as a technique for civil engineering structures and buildings. In the method for civil engineering structures, weighting factors for earthquake motion characteristics are provided for interplate and inland earthquakes. The weighting factor for an interplate earthquake consists of five coefficients, C_1 to C_5 (Iwasaki et al, 1978), and the weighting factor for the irregular nature of an earthquake motion is C_2. C_2 has been determined using uniform loose sand that did not contain fine-grained soil (Ishihara and Yasuda, 1975); it value is 1/0.55 to 1/0.70. Subsequent experiments determined that this weighting factor changes with the density of the sand (Tatsuoka et al. 1986). The wave forms used for the previous experiment were from 1964 Niigata earthquake, the 1968 Tokachi-oki earthquake, and the 1978 Miyagi-ken-oki earthquake, and the duration of earthquake motion was short compared with the 2011 Great East Japan Earthquake. It is expected that the result for a huge interplate earthquake would show increased danger. Therefore, the authors (2014) reappraised C_2 by considering fine fraction and density using the cyclic torsional shear test and the wave form of the Great East Japan earthquake (as observed in Urayasu). Compared with the C_2 from previous studies, a 20 to 30 percent deterioration in strength was confirmed due to the effect of long duration seismic waves.

The objective of this study was to perform reasonable prediction of a huge interplate earthquake, including the seismic effects of long duration and the regionality of liquefaction strength using representative soil profile models created from existing ground survey results. In relation to the Great East Japan Earthquake, the prediction results were compared to the liquefaction damage at Urayasu. The effectiveness of this prediction method was assessed.

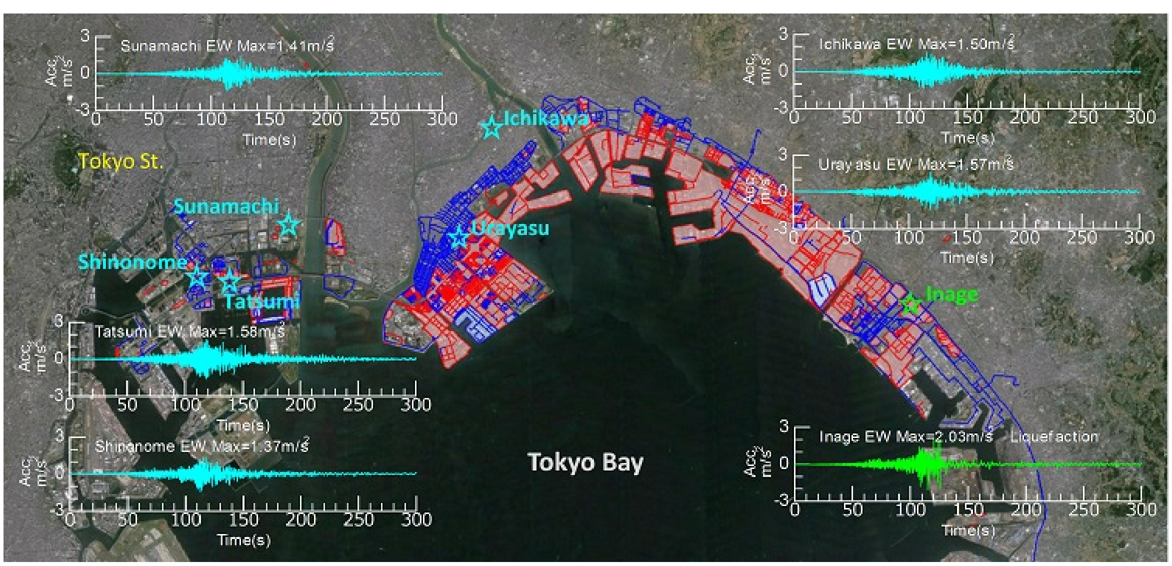

Fig.1 Liquefaction area and observed earthquake motion of the Tokyo Bay area, by K-NET

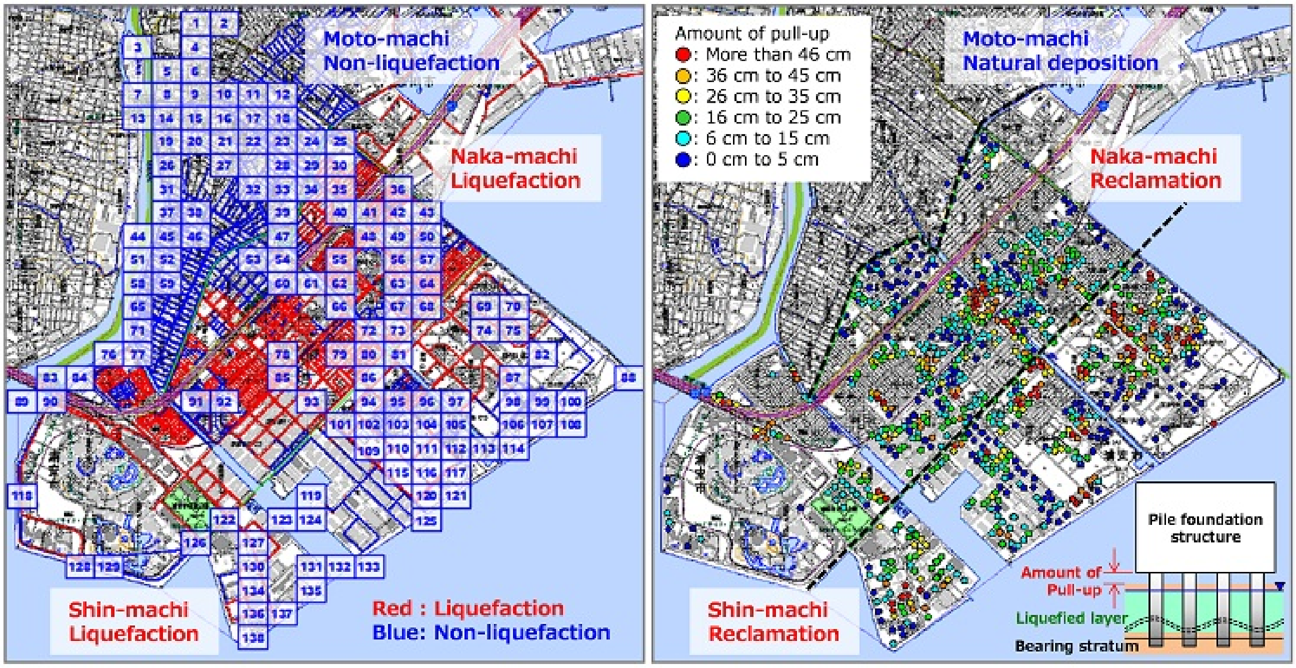

Fig.2 Meshes where RPSMs were constructed for Urayasu, and liquefaction-induced ground displacement

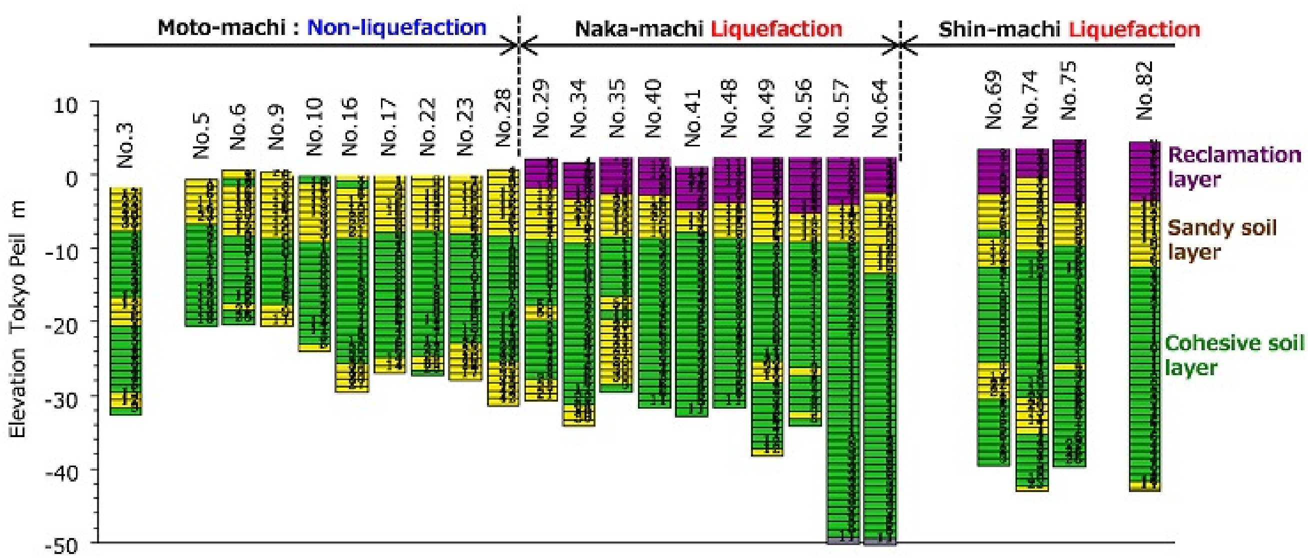

Fig.3 Representative soil profile models

2. Ground characteristics and the liquefaction damage at Urayasu

The mesh positions that created the Representative Soil Profile Models in Urayasu are shown in Fig.2. The ground model equalizes the boring data in 250 m meshes. Moto-machi is a natural deposition ground, whereas Naka-machi and Shin-machi are reclaimed land. Modeling of the topography boundary region of Moto-machi and Naka-machi compared the area ratio of natural deposition ground and reclaimed land and created a representation ground model with boring data over a larger area. The ground model of the region north and south of Urayasu is shown in Fig.3, where Moto-machi is No.3 to No.28, Naka-machi is No.29 to No.64, and Shin-machi is No.69 to No.82, and a mesh number corresponding, respectively. The stratum at Naka-machi and Shin-machi were deposited in the following order: reclamation layer (F), alluvial-sand layer (As), and alluvial cohesive soil layer (Ac). The F layer has a thickness of 4 to 8 m, and the As layer has a thickness of 3 to 10 m; the Ac layer is very thick.

According to Yasuda et al. (2012), a field survey was performed the day after the earthquake; the occurrence of liquefaction in Urayasu, is shown in Fig. 2. In this figure, a red line shows points where sand boil was confirmed and a blue line shows points where sand boil was not confirmed. In the reclaimed land of Naka-machi and Shin-machi, sand boil, which is a liquefaction trace, was mostly confirmed for the whole region; whereas, this liquefaction trace was not confirmed on the natural deposition ground in Moto-machi. According to Chiba Prefecture (2011), the liquefaction-induced settlement damage was investigated and this amount of displacement was summarized as the difference between the ground displacement and the pile foundation. Moto-machi is a non-liquefied area and liquefaction-induced settlement was not confirmed. However, Naka-machi and Shin-machi are liquefaction areas, with a liquefaction-induced settlement of 5 to 25 cm (maximum of 95 cm). Field survey results show that the main layers liquefied by this earthquake were reclamation layers.

3. Liquefaction prediction by a Representative Soil Profile Models

3.1 Method of liquefaction prediction

The method of liquefaction prediction used in this study is the safety factor against liquefaction (F_{L}) method, the safety factor against liquefaction, which is used for making a general liquefaction hazard map in Japan. The study conditions for the liquefaction prediction are shown in Fig.4. Case 1-1 is a judgment result using the conventional method, according to Japan Road Association (2012). Case 1-2 added the effect of a long duration earthquake motion to Case 1-1. Case 1-3 added an aging effect of ground generation of the As layer to Case 1-2. Case 2-2 added the effect of a long duration earthquake motion to Case1. Case 2-3 added the effect of aging of the As layer. Calculation conditions were as follows.

1) The *N* value was set to the value of each depth of a Representative Soil Profile Model.

2) The fine-fraction content (F_{C}) was established by the relationship between N_1 and F_{C} from the results of an investigation of Urayasu City (2011).

3) The liquefaction strength ratio was established by the method of Japan Road Association (JRA method) and a method that considers the regionality of the Tokyo lowlands (TG method) by Kamei et al (2002). The JRA method is an estimated equation considered in relation to the whole of Japan, whereas the TG method is an estimated equation specific to the alluvial-sand layer of the Tokyo lowlands. In addition, Urayasu City (2011) conducted a detailed ground survey after the earthquake and determined for the liquefaction strength using the undisturbed experimental samples. It was confirmed that the F layer is congruous with the TG method and that the As layer is congruous with 1.2 times increase in the TG method.

4) The weighting factor for an interplate earthquake is set up based on two approaches: the conventional weighting factor of 1.0 given by the JRA method and a weighting factor that the authors determined experimentally based on the ground motion waveform of Urayasu.

5) The aging effect of an alluvial-sand layer is set to 1.4, according to Towhata et al (2014).

6) The groundwater level is the mean value of the results of an investigation in each mesh.

7) The earthquake external force is set to 200 cm/s^2, which is the mean value of the maximum acceleration of each component based on nine observation records in the area of Naka-machi and Shin-machi. For Moto-machi, it was set into 174 cm/s^2, which is the composite acceleration of observation records at K-NET Urayasu.

3.2 Results of liquefaction prediction

From the liquefaction prediction results for each study condition, Liquefaction Potential Index, *LPI*, distribution maps are shown in Figures 5-10. The 250-m mesh, which carried out liquefaction prediction, Moto-machi is 32 meshes, Naka-machi is 43 meshes, and Shin-machi is 40 meshes. Meshes without hatching were excluded from this study because they had an unknown groundwater level or were ocean space where the ground surface

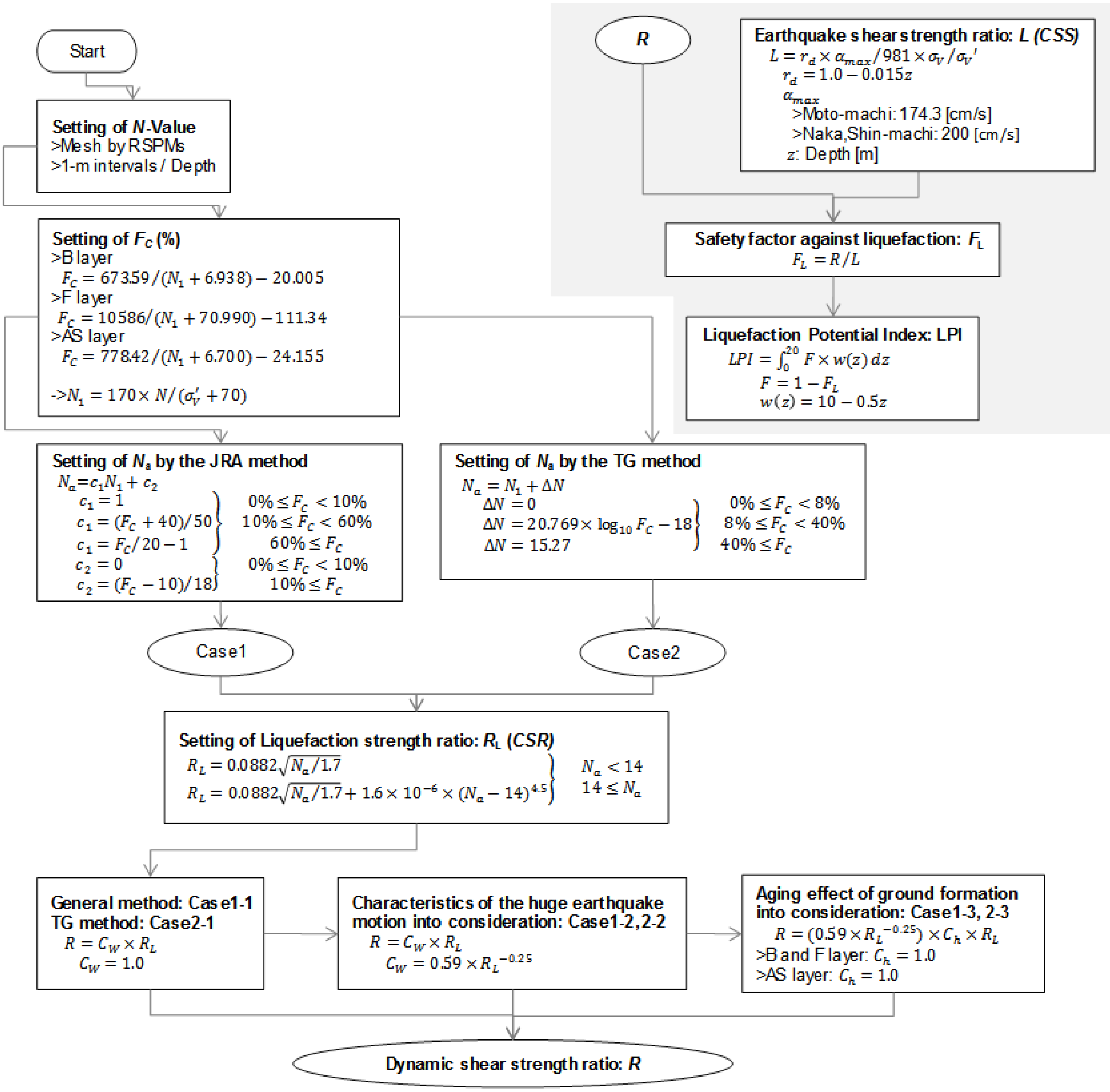

Fig.4 Flow chart of the liquefaction judgments

elevation is less than 0 m. The *LPI* is an index that grades of the severity of liquefaction; it was devised by Iwasaki et al (1978). This index is the result of finding the integral in the depth direction against F_L, which is less than 1.0. The formula for the *LPI* is shown in Figure 4. It is classified into four ranges, A to D, as follows: *LPI* =0 (A-range), for which the hazard of liquefaction is considerably low; *LPI* = 1− 5 (B-range), for which the hazard of liquefaction is low; *LPI* = 6− 15 (C-range), for which the hazard of liquefaction is high, and *LPI* > 15 (D-range), for which the hazard of liquefaction is extremely high.

Case 1-1 (Fig.5) is the decision result obtained using the JRA method. This is the general judgment result used for liquefaction prediction in Japan. At a distribution ratio of *LPI* for Moto-machi, the mesh within the A-range dominates, occupying 85%; the C-range occupies the remaining 15%. In Naka-machi, the B-range is 19%, the C-range is 42%, and the D-range is 39%. In Shin-machi, the B-range is 3%, the C-range is 23%, and the D-

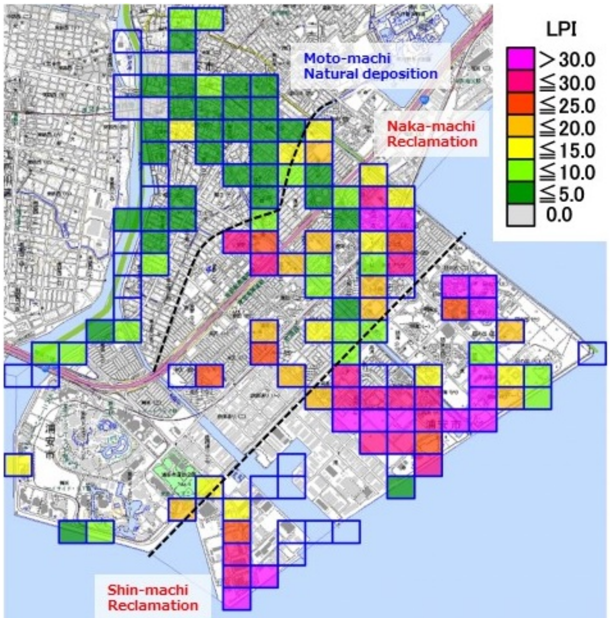

Fig.5 Distribution of *LPI*, estimated by Case 1-1

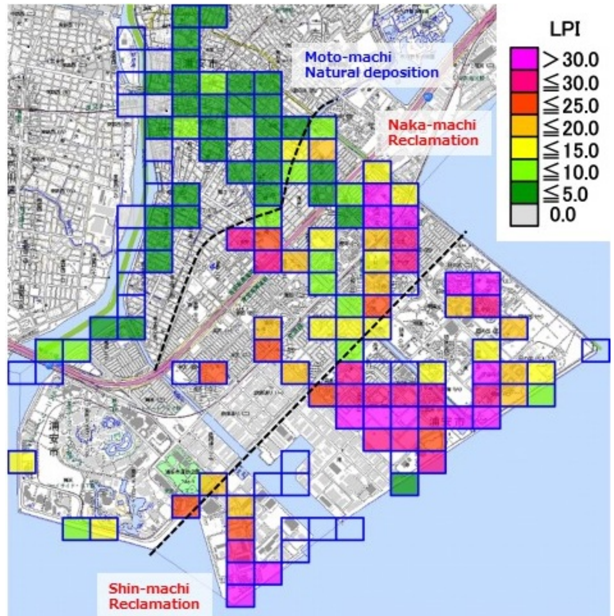

Fig.6 Distribution of *LPI*, estimated by Case 1-2

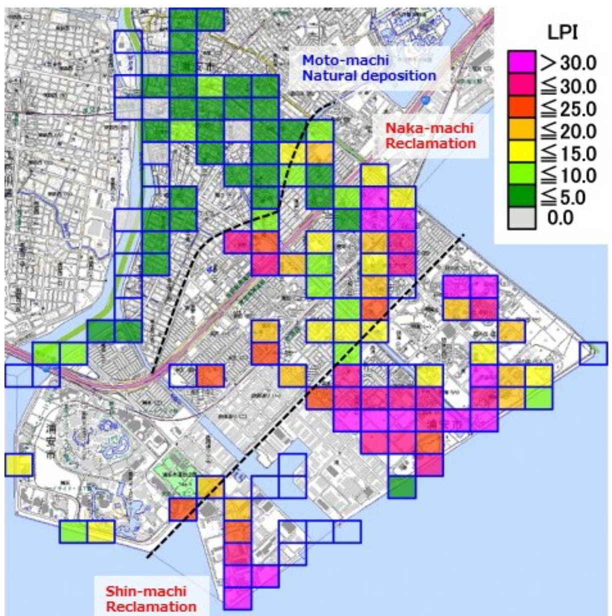

Fig.7 Distribution of *LPI*, estimated by Case 1-3

range is 74%. When the actual situation was compared with the prediction result, liquefaction was not occurred in Moto-machi, it will be considered that liquefaction is not occurred and that an evaluation result is therefore too safe. Moreover, the mean *LPI* value of liquefaction areas in Naka-machi and Shin-machi is 20. Many meshes in the D-range are confirmed and it can consider the possibility of safety as well as the judgment result of Moto-machi.

Case 1-2 (Fig.6) is the decision result having added the effect of the earthquake motion characteristics to Case 1-1. The *LPI* increases about threefold compared with Case 1-1. In Moto-machi, the B-range dominates, with 38%, and the C-range occupies 24%. This evaluation shows a high risk of liquefaction in more than a half of the meshes. It also yields a different result from the actual phenomenon.

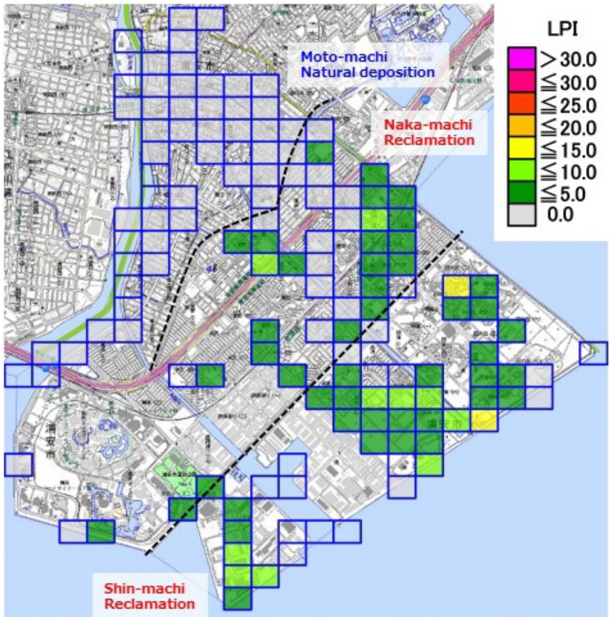

Fig.8 Distribution of *LPI*, estimated by Case 2-1

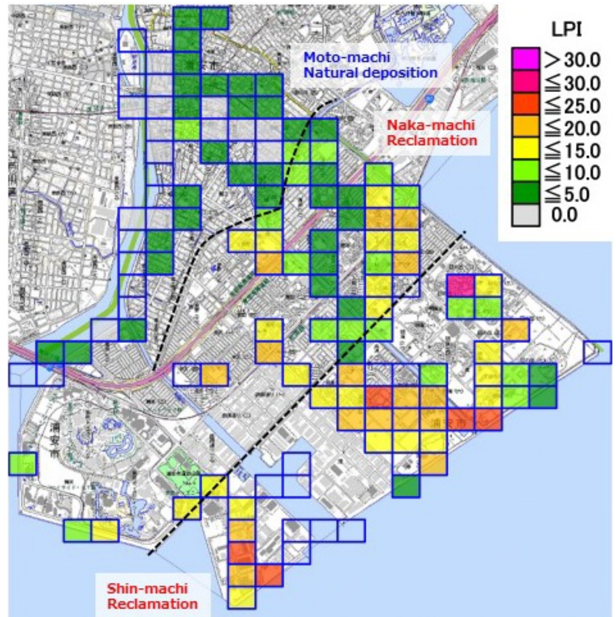

Fig.9 Distribution of *LPI*, estimated by Case 2-2

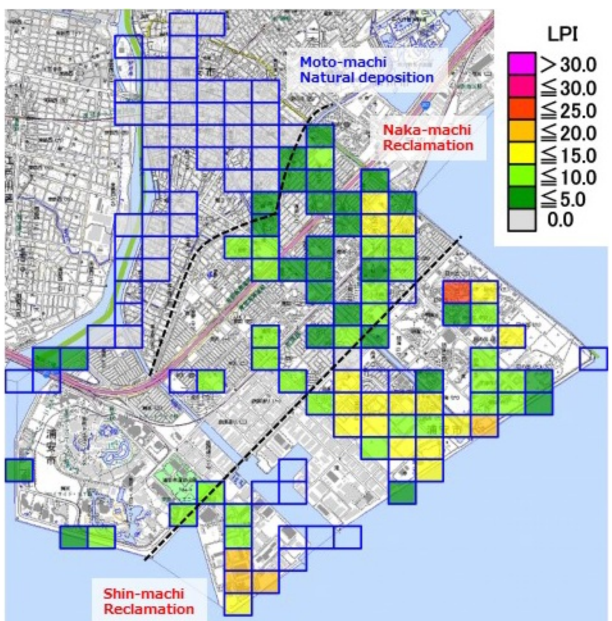

Fig.10 Distribution of *LPI*, estimated by Case 2-3

Case 1-3 (Fig.7) is the decision result having added the aging effect of ground formation to Case 1-2. Compared with Case 1-2, the *LPI* decreases about 30 percent at Naka-machi and Shin-machi. In Moto-machi, which has natural deposition ground, the B-range dominates, with about 94%, and the C-range decreases from about 24% to about 6%. These results are considered to be close to the actual situation. As mentioned above, it is considered that this is an evaluation of excessive safety compared with the actual phenomenon.

Case 2-1 (Fig.8) is the decision result from the TG method. Compared with the JRA method, we would expect an increase in the liquefaction strength when using the fine fraction; therefore, *LPI* decreased compared with Case 1-1. All of the meshes in Moto-machi were in the A-range. In Naka-machi, the B-range occupies about 95% and the C-range occupies about 5%. In Shin-machi, the B-range occupies about 75% and the C-range

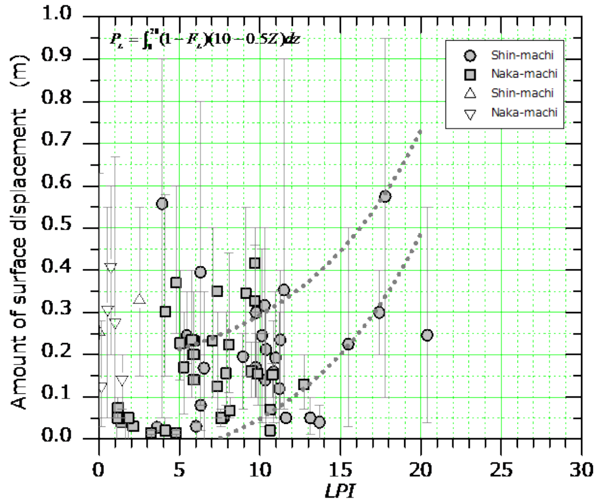

Fig.11 Relationship between *LPI* and ground displacement in Case 2-3

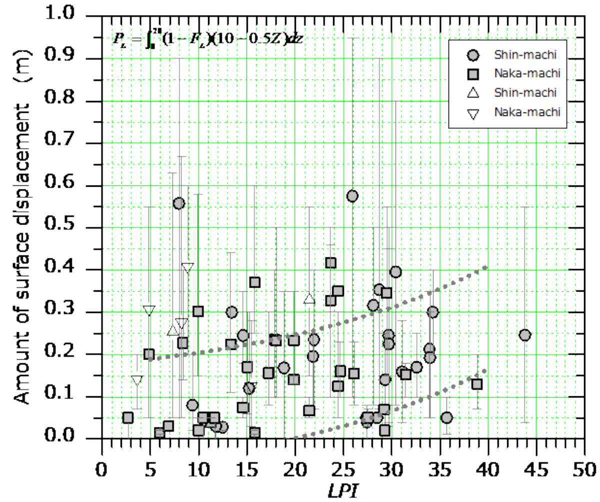

Fig.12 Relationship between *LPI* and ground displacement in Case 1-1

occupies about 25%. The *LPI* of the liquefied area of Naka-machi and Shin-machi averages approximately 2, and the hazard from liquefaction is low; this is considered to be a risky evaluation.

Case 2-2 (Fig.9) is the decision result having added the effects of the earthquake motion characteristics to Case 2-1. Compared with Case 2-1, the *LPI* increases in all meshes. In Moto-machi, the B-range dominates, occupying about 97%, and the C-range occupies about 3%. In Naka-machi, the B-range occupies about 35%, the C-range occupies about 52%, and the D-range occupies about 13%. In Shin-machi, the B-range occupies about 10%, the C-range occupies about 48%, and the D-range occupies about 42%. The *LPI* of the liquefied area of Naka-machi and Shin-machi averages approximately 10. The liquefaction hazard is considered high; the *LPI* is about half that of Case 1-2.

Case 2-3 (Fig.10) is the decision result having added the aging effect of ground formation to Case 2-2. Compared with Case 2-2, the *LPI* decreases about 40 percent at Naka-machi and Shin-machi. In Moto-machi, with natural deposition ground, the whole region fell into the A-range. In Naka-machi and Shin-machi, where there are liquefied areas, the C-range occupied about 61% and the *LPI* averaged 7. Compared with Case 1-3, the D-range mostly disappears. This is considered to be the judgment result most closely predicting the actual situation. In the judgment results of Naka-machi and Shin-machi, it is considered that the ground model of the A-range has a groundwater level as deep as 3 m below the surroundings; the *LPI* value is underestimated due to this effect.

The relationship between the *LPI* from Case 2-3 (considered consistent with the actual damage) and actual surface displacement (Fig.2) is shown in Fig.11. The relationship between the *LPI* from Case 1-1 and actual surface displacement is shown in Fig.12. The actual amount of surface displacement is the mean value in each mesh (approximately the amount of relative pull-up of the pile foundation in Fig.2), and the error bars show the maximum to minimum range. At Naka-machi and Shin-machi, there is a tendency for surface displacement to increase with the *LPI*. Surface displacement occurred when the *LPI* exceeded about 5, where the value of surface displacement was 10 cm or more. The dotted line in the figures shows the range of the data about the mean, i.e., plus or minus one standard deviation. The approximate values of surface displacement are follows: *LPI* =5 is 0.0 − 0.20 m, *LPI* =10 is 0.05− 0.30 m, and *LPI* =15 is 0.20− 0.45 m. The triangle symbols show remarkably low *LPI* values and represent data different from the field investigation. For a surface displacement that is less than the lower limit of the dotted line can think of a possibility of including the place which used the pile foundation and a ground improvement together. For the general method in Case 1-1, the *LPI* becomes large and the amount of ground displacement due to the difference in the *LPI* does not differ greatly.

3.3 Potentiality judgment of the liquefaction damage of residential land

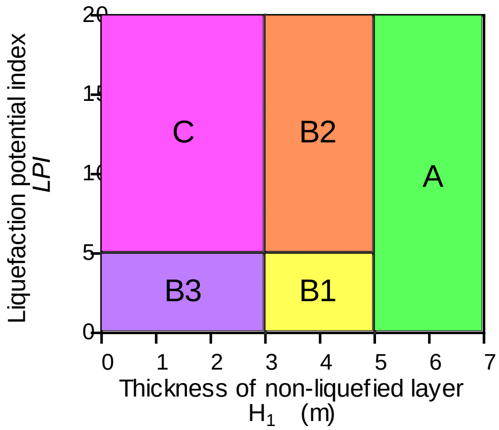

Class	Probability of liquefaction-induced damage
C	High
B3	Comparatively low
B2	
B1	
A	Low

Fig.13 Probability banks for liquefaction-induced damage to houses by *LPI* and H_1

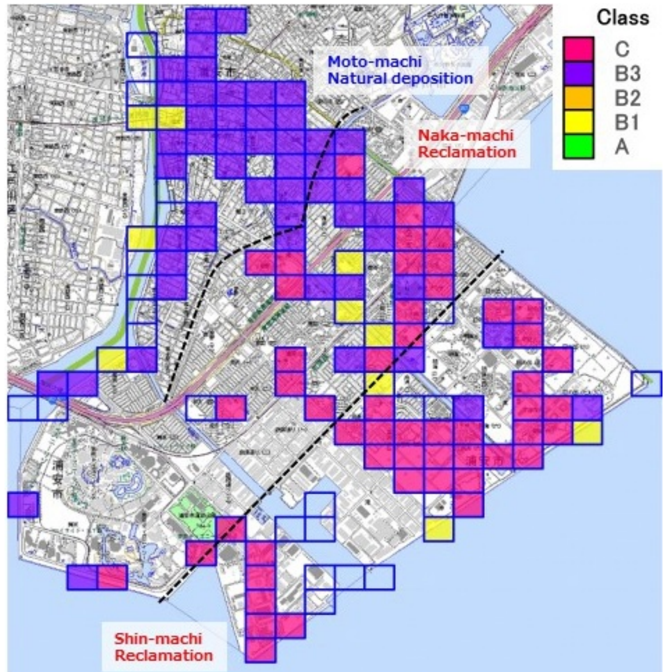

Fig.14 Hazard map for potential damage to wooden houses based on the new criterion proposed by MLIT

The new criterion to estimate the liquefaction-induced damage to wooden houses was proposed in 2014 by MLIT based on case studies of houses that were damaged and houses that were not damaged during the 2011 Great east japan earthquake. Fig.13 shows the new criterion, in which the possibility of damage can be estimated by *LPI* and the thickness, H_1, of the non-liquefied layer overlaying the liquefied layer. This technical guideline is judged against the result of Case 2-3 and is shown in Fig.14.

The LPI of Moto-machi is <5 and is a judgment result of B3 or B1 due to the difference in groundwater level. For Naka-machi and Shin-machi, which are liquefaction areas, about 61% of the mesh is a C judgment. This confirms the C judgment, even in residential areas, which indicates serious liquefaction damage to timber housing.

4. Conclusions

In this study, a reasonable prediction method for the liquefaction hazard map of a huge interplate earthquake using Representative Soil Profile Models was devised based on the liquefaction situation of the 2011 Great East Japan Earthquake. The following conclusions were derived from the study.

When a liquefaction strength ratio is estimated, it is very important to respond for each examination area, to determine for the relationship between N value and fine-fraction content, and to take regionality into consideration. Because the Great East Japan Earthquake was huge (M_W = 9.0), the duration of shaking was very long; therefore, the correction factor C_2 must be modified in the estimation of the safety factor against liquefaction. By setting this up appropriately, it is considered that an evaluation result was obtained that was almost consistent with the actual damage situation.

The potential for damage to houses must be evaluated not only using the soil liquefaction potential index, *LPI*, but also from the thickness of the non-liquefied layer, H_1, as proposed by the MLIT of Japan. The hazard map based on *LPI* and H_1 coincides well with the zones where wooden houses were severely damaged during the 2011 Great East Japan Earthquake.

Acknowledgements

The ground motion waveform was allowed to use an observation result in National Research Institute for Disaster Prevention K-NET. Some of the results cited in this paper are quoted from a report by the technical committee on measures against liquefaction, chaired by Prof. Ishihara and organized by the Urayasu City Government. Furthermore, the precious field investigation record by Chiba Prefecture was also cited. The Representative Soil Profile Models was created by joint efforts of the students of Tokyo Denki University. The authors would like to express their sincere appreciation to all of them.

References

[1] National Research Institute for Earth Science and Disaster Prevention (NIED): K-NET WWW service. Japan, http://www.kyoshin.bosai.go.jp/kyoshin/ (2011.4)

[2] Iwasaki T, Tatsuoka F, Tokida K, and Yasuda S (1978): A practical method for assessing soil liquefaction potential based on case studies at various sites in Japan. Proc. 2nd international conference on Microzonation, San Francisco, USA, Vol.2, 885-896.

[3] Ishihara K, and Yasuda S (1975): Undrained deformation and liquefaction of sand under cyclic stress. Soils and Foundations, 15 (1), 45-59.

[4] Tatsuoka F, Maeda S, Ochi K, and Fujii S (1986): Prediction of cyclic undrained strength of sand subjected to irregular loading, Soils and Foundations, 26 (2), 73-90.

[5] Ishikawa K, Yasuda S, and Aoyagi T (2014): Studies on the reasonable liquefaction-prediction method of the 2011 Great East Japan Earthquake. Japanese Geotechnical Journal, 9 (2), 169-183. (in Japanese).

[6] Yasuda S, Harada K, Ishikawa K, and Kanemaru Y (2012): Characteristics of liquefaction in Tokyo Bay area by the 2011 Great East Japan Earthquake. Soils and Foundations, 52 (5), 793-810.

[7] Chiba Prefecture (2013): Archives of the 2011 Great East Japan Earthquake. Japan, https://www.pref.chiba.lg.jp/bousaik/jishin/kirokusi/kirokusi.html. (2016.04.14)

[8] Japan Road Association (2012): Specification for Highway Bridges. Maruzen. (in Japanese).

[9] Technical Committee on Measures Against Liquefaction in Urayasu City (2011): Report on rmeasures against liquefaction in Urayasu City. http://www.city.urayasu.lg.jp/shisei/johokoukai/shingikai/shichoukoushotsu/1002796/1002934.html (in Japanese)

[10] Kamei M, Morimoto I, Yasuda S, Shimizu Y, Koganemaru K, and Ishida E (2002): A consideration on grain size of alluvial sands and relationships between fines and liquefaction resistance in Tokyo lowland. Journal of Japanese Geotechnical Society, 42 (4), 101-110.

[11] Towhata I, Goto S, Taguchi Y, Hayashida T, Shintaku Y, and Hamada Y (2015): On ageing of liquefaction resistance of sand. Proc. 15th Asian Regional Conference on Soil Mechanics and Geotechnical Engineering, Fukuoka, Japan, JPN-072.